



Vol. 5, No. 2 December 2011

DFI JOURNAL

The Journal of the Deep Foundations Institute

PAPERS

Themed Edition on Testing:

Case History: Foundations for the New Mississippi River Bridge, St. Louis – Paul J. Axtell and Dan A. Brown [3]

Geotechnical Exploration Phase Drilled Shaft Load Testing – Walter E. Vanderpool, Rick L. Chesnut and Michael E. McGettigan [16]

Lateral Load Testing Micropiles to Evaluate the Impact of Threaded Joints and Casing Embedment on Short Micropiles in Shallow Rock – J. Brian Anderson and Michael R. Babalola [23]

Hyperbolic P-Y Model for Static and Cyclic Lateral Loading Derived from Full-Scale Lateral Load Testing in Cemented Loess Soils – Steven Dapp, Dan A. Brown and Robert L. Parsons [35]

Determination of Pile Damage in Concrete Piles – Gerald E.H. Verbeek and Peter Middendorp [44]

TECHNICAL NOTE

Hollow Threaded Rebar for Cross Hole Sonic Logging Access Tubes Combined with Longitudinal Concrete Reinforcing in Drilled Shafts – Josef K. Alter [51]

Deep Foundations Institute is the Industry Association of Individuals and Organizations Dedicated to Quality and Economy in the Design and Construction of Deep Foundations.

Case History: Foundations for the New Mississippi River Bridge, St. Louis

Paul J. Axtell, Dan Brown and Associates, Overland Park, Kansas, USA;
paxtell@danbrownandassociates.com

Dan A. Brown, Dan Brown and Associates, Sequatchie, Tennessee, USA;
dbrown@danbrownandassociates.com

ABSTRACT

This case history describes the foundation design and construction for the New Mississippi River Bridge, presently under construction in St. Louis, Missouri. The 1,500 ft (457.2 m) main span of the cable-stayed bridge is supported by two delta tower pylons in the river, with anchor piers on each bank. The final foundation design was completed as a part of an Alternate Technical Concept (ATC) proposal by the winning construction team, and utilized drilled shafts up to 11.5-ft (3.5-m) diameter that were socketed into very hard limestone. As part of the ATC foundation design, a full-scale, bi-directional static load test was performed to verify the design and allow use of higher resistance values. This paper presents the results of the site exploration, construction of the load test shaft, details of the load testing, and a comparison of the test results with various design parameters.

INTRODUCTION

A dual-tower cable-stayed bridge over the Mississippi River, shown in Fig. 1, is being constructed by a joint venture comprised of Massman, Traylor Brothers, and Alberici (MTA). The project is referred to as the New Mississippi River Bridge (MRB) and is located in Missouri and Illinois, just north of downtown St. Louis. This bridge, along with several other approach construction contracts, will carry traffic along I-70 over the river and is intended to significantly reduce traffic congestion in the area. The main span of the bridge is 1,500 ft (457.2 m) and each back span is 635.75 ft (193.8 m) for a total bridge length of 2,771.5 ft (844.8 m). The project was designed by HNTB for the Missouri Department of Transportation (MoDOT), who is administering the construction contract.

As part of the project procurement process, the owner allowed pre-bid Alternate Technical Concepts (ATC's) to be submitted by pre-qualified construction teams. One such ATC that was offered and accepted included a re-design of the drilled shaft foundations. The ATC foundation design utilized the construction team's ability to construct larger individual foundation elements, thereby reducing the overall size of the cofferdam and footing. A full-scale load test on a non-production drilled

shaft was included in the ATC in order to allow the use of higher resistance factors in the LRFD design approach.

Major factors affecting the design of the foundation included lateral and overturning forces from wind load, vessel collision forces, and seismic demands. In addition, deep scour conditions resulted in unsupported length of up to 66 ft (20.1 m) between the base of the cap and the top of rock.

At each pylon, the resulting ATC foundation design reduced the number of drilled shafts from fourteen to six, although the diameter of the shafts increased to 11.5 ft (3.5 m) from 10 ft (3.05 m). The ATC also allowed the pylon pile caps to be reduced in plan size to 88 ft (26.82 m) by 55 ft (16.76 m) from 120 ft (36.58 m) by 70 ft (21.34 m); the pylon cofferdam seals were also reduced accordingly. At Pier 11 (Missouri Pylon), the ATC design rock socket length was reduced to 22 ft (6.71 m) from 44 ft (13.41 m); at Pier 12 (Illinois Pylon), the ATC design rock socket length was reduced to 16.5 ft (5.03 m) from 44 ft (13.41 m). Beneath the anchor piers, the baseline drilled shaft diameter was maintained at 10 ft (3.05 m) in the ATC because each shaft supports an individual column. However, the ATC design reduced the rock socket lengths to 14.25 ft (4.34 m) from 28 ft (8.53 m).

Top of Rock Elevation: <u>319</u> Completion Date: <u>2/16/10</u>		GRAPHIC LOG	SAMPLES
Datum <u>msl</u>			
DEPTH IN FEET	DESCRIPTION OF MATERIAL	DRY UNIT WEIGHT (pcf) SPT BLOW COUNTS CORE RECOVERY/RQC	
0-5	Hard, gray, very finely crystalline, thick bedded, fresh LIMESTONE with chert nodules clay seam from 1.7 to 1.8 feet Unconfined Compressive Strength = 26,592 psi	100% 77%	NX1
5-10	Unconfined Compressive Strength = 29,829 psi	100% 88%	NX2
10-15	Unconfined Compressive Strength = 22,616 psi moderately hard, slightly pitted from 9.4 to 9.9 feet	100%/100%	NX3
15-20	Unconfined Compressive Strength = 21,919 psi	100% 100%	NX4
20-25	Unconfined Compressive Strength = 19,767 psi	100% 100%	NX5
25-30	clay seam (0.25 inches)	100% 100%	NX6
30-35	with shale partings from 29.0 to 29.4 feet with shale partings from 30.7 to 31.5 feet	100% 100%	NX7
35-40		100% 94%	NX8
40-45		100% 100%	NX9
45	shale seam from 43.0 to 43.2 feet Boring terminated at 44 feet.	100% 100%	NX10

[FIG. 2] Boring Log at Test Shaft Location (1 ft = 0.3 m and 1 psi = 6.9 kPa)

The potential for solution cavities within the limestone was a significant concern for the project. A substantial cavity was detected at the location of a pylon foundation for an earlier preliminary design for the bridge where a longer main span was considered; however, at the present and final location of the pylons, no significant solution cavities were detected.

In addition to conventional coring, additional information was obtained from the boreholes using an Acoustic Televiewer (ATV) at each exploratory hole that was cored. A more detailed discussion of the results of the ATV, along with a description of the technology and its application, are provided by Keller (2010). Although the concern for solution cavities was a motivating factor for the use of the ATV investigation, the ATV proved to be beneficial to the construction operations. The constructor was able to utilize the ATV information to identify seams or horizontal fractures within the bedrock. The rock excavation within the

drilled shaft was performed using coring tools and the constructor successfully utilized the existing seams identified by the ATV logs to plan the core breaks and recover cores efficiently. The graphical output from the ATV investigations agreed very well with coring information, namely recovery and RQD, and also agreed very well with visual observation of the recovered cores during shaft construction. Examples of ATV logs are shown on Fig. 4, illustrating the horizontal seam/fractures that were noted at elevation 311.7 ft and 306.0 ft (95.0 m and 93.3 m).



[FIG. 3] Test Shaft Boring Recovered Rock Core

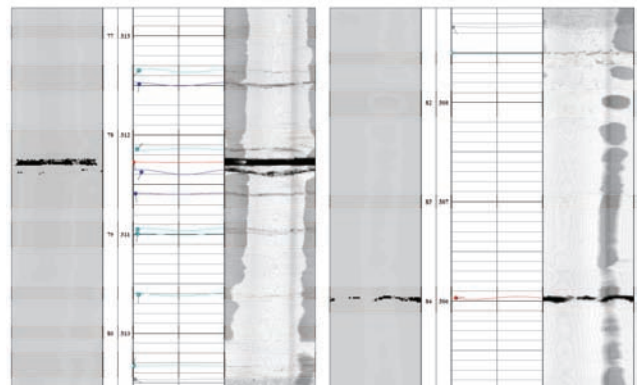


[FIG. 4] ATV Logs from Load Test Location

The bedrock encountered at the location of the test shaft is representative of the conditions found at Piers 11, 12, and 13 with respect to recovery, RQD, and unconfined compressive strength. The bedrock at Pier 10 exists at higher elevations than Piers 11, 12, and 13 and the conditions there are slightly less favorable with respect to RQD.

Unconfined compression tests on the rock cores at the test shaft location indicate that the strength of the rock was extremely high, and exceeded the compressive strength of the concrete. Five unconfined compression tests were performed on rock core recovered from the investigative boring at the location of the test shaft, as indicated on the boring log in Fig. 2 and shown graphically in Fig. 5. The average value of the five tests is 24,145 psi (166 MPa) and ranges from 19,767 psi (136 MPa) to 29,829 psi (206 MPa). Other test data from nearby Pier 11 are also shown, and these data suggest that the rock at the load test location had similar characteristics to the nearby pylon location. The data show a slight trend of decreasing strength with depth.

An inconsistency was noted with respect to the measured unconfined compressive strengths; as evident on Fig. 6, the values reported from borings provided prior to bid (design phase) were significantly lower than those obtained during the post-award investigation (construction phase). The writers had no involvement in the design phase investigation and can only speculate that such a discrepancy may result from sampling technique, sample transportation, or test sample preparation.

A small portion of the construction-phase drilling operation and laboratory procedures were observed by the primary author. In all instances, recovered construction-phase core samples were tested within 24 hours of recovery. Upon discovering the apparent discrepancy between design- and construction-phase strengths, MoDOT independently tested some of the remaining construction-phase samples. These reported values, also shown in Fig. 6, do not appear to differ significantly from the construction-phase values reported by MTA, although they do exist at the lower range of the measured values. MoDOT also tested some of the remaining design-phase cores that had been in storage for approximately 1 year, the results of which are also shown in Fig. 6.

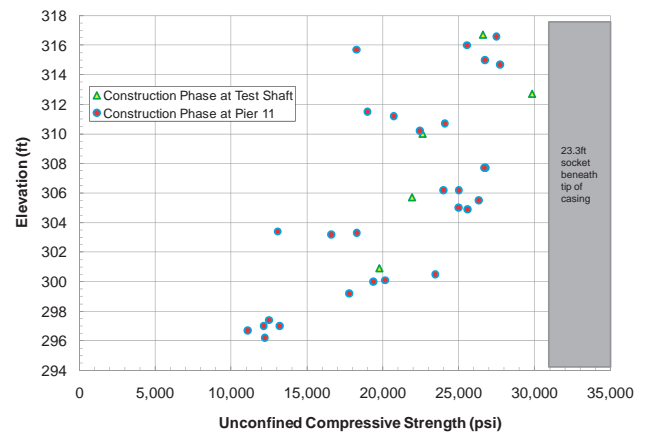


[FIG. 5] Bedrock Unconfined Compressive Strength at Test Shaft (1 psi = 6.9 kPa)

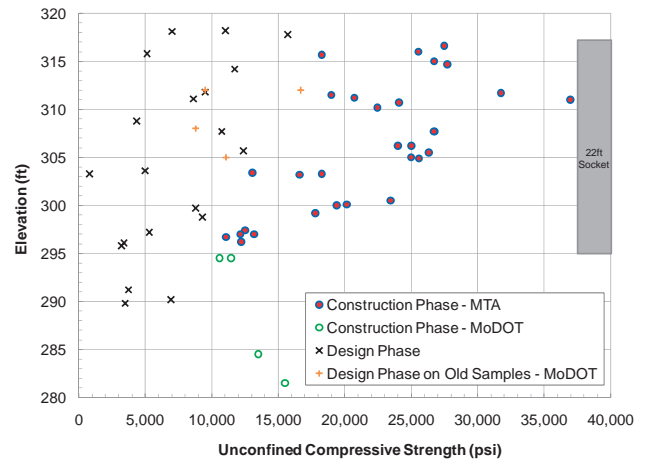


[FIG. 6a] Bedrock Unconfined Compressive Strength at Pier 11 (1 psi = 6.9 kPa)

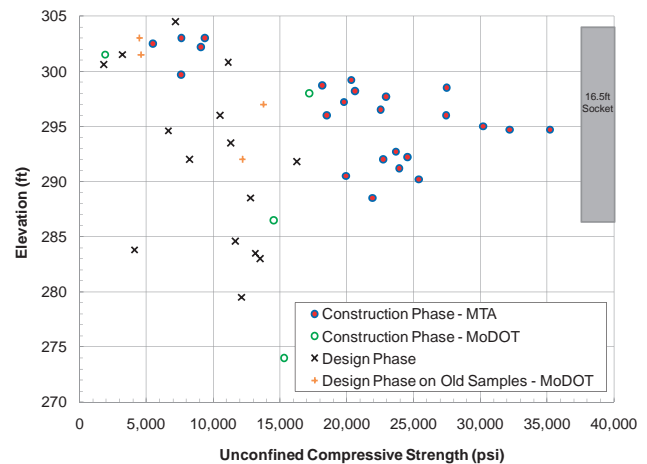


[FIG. 6b] Bedrock Unconfined Compressive Strength at Pier 12 (1 psi = 6.9 kPa)

The differences in pre-bid vs post-award measurements of rock strength are potentially significant from a contractual perspective, since this discrepancy opens the possibility for a claim of a differing site condition (DSC) by the constructor. If the higher strength results in a material difference in the production rates

achieved in excavation of the drilled shafts compared to the estimate used in the bid, then the contractor may be entitled to additional compensation. Contract requirements to provide timely notice of a potential DSC dictated that the contractor notify the owner of the difference. However, the constructor's means and methods subsequently proved to be effective in drilling the rock at the pylon locations and the difference was not determined to significantly affect the work.

While the reason(s) for the differences in unconfined compression strength are not known, the construction-phase tests are considered the more reliable indicator due to the writer's direct knowledge of the sampling and testing procedures. Accordingly, based on Figs. 4 and 5, the average unconfined compressive strength contributing to the side resistance is considered to be 24,000 psi (165 MPa) for the test shaft. The unconfined compressive strength in the vicinity of the base of the test shaft is considered to be 12,000 psi (83 MPa).

TEST SHAFT CONSTRUCTION

A load test was performed using four bi-directional embedded jacks (Osterberg Cell, or O-cell) to load the base of the shaft against the side resistance of the socket above the base. A full size test shaft was constructed in order to demonstrate the contractor's ability to construct the drilled shafts and to verify the design values of side and base resistance on a drilled shaft constructed using means and methods which are identical to those used on production foundations.

The test shaft was constructed in the river just north (upstream) of Pier 11. The permanent casing was set on Tuesday, May 4, 2010 and rock socket excavation with a core barrel began May 5, 2010. Drilling was completed on May 13, 2010. Shortly after the rock socket excavation was completed, the Mississippi River level rapidly increased and inundated the permanent casing. Work was suspended until June 1, 2010, at which time the river level receded to a point in which work could resume.

While test shaft construction work was suspended due to elevated river levels, a barge inadvertently collided with the permanent casing that was submerged. When the river receded, the top of the permanent casing was

observed to be slightly deformed and required removal of about 1.5 ft (0.46 m) of casing on the southern one-third of the circumference. Inspection of the diameter and alignment along the full length of the casing and shaft excavation was performed using a downhole sonic caliper device that utilizes real-time sonar technology to provide a 360 degree profile of the shaft at discrete levels. A three-dimensional model of the shaft excavation was generated that indicated that the casing was unaffected by the barge impact beneath a depth of about 20 ft (6.1 m), and therefore did not affect the load test of the rock socket.

Because of the delay between excavation and concrete placement, a "back-scratch" tool, similar to a wire brush, was used to remove any loose material that may have accumulated on the socket walls. This procedure occurred prior to the final clean-out and inspection of the shaft. Because the steel cables extending from the back-scratch tool are flexible and the rock is relatively hard, no enhancement to side resistance is estimated to result from the back-scratching operation, other than the benefit gleaned from exposing clean rock prior to receiving concrete.

The test shaft was constructed in the following manner, the details of which are discussed below:

1. A 13-ft (3.96-m) diameter starter casing was installed with a vibratory hammer to a tip depth about 20 ft (6.1 m) beneath the riverbed.
2. The starter casing was then charged with bentonite slurry, from the bottom up so the river water was displaced;
3. A 12.5-ft (3.81-m) diameter hole was drilled through the soil overburden to the top of rock under bentonite slurry using a vented drilling bucket with auger flights welded to the outside;
4. An 11.5-ft (3.51-m) diameter, 91.5-ft (27.9-m) long permanent casing was installed in the open hole and seated into rock by twisting it with the drill rig. The permanent casing had carbide teeth at the tip and was advanced about 2.6 ft (0.79 m) with the drill rig. The top of the permanent casing was at Elevation 409.1 ft (124.7 m). Based on observed differential water head elevations inside and outside of the permanent casing, it appears a positive seal was mostly achieved and maintained;
5. The bentonite slurry was exchanged with

river water by pumping the slurry from the bottom of the hole, through the de-sanding plant, and back to the storage tanks. River water was added at the surface to replenish the fluid;

6. An 11-ft (3.35-m) diameter, 23.3-ft (7.1-m) long rock socket was drilled using a core barrel and core extractor (socket length measured from tip of permanent casing). Using a weighted tape, the average depth to the base of the shaft from the top of the permanent casing was about 114.8 ft (35.0 m);

7. The permanent casing and rock socket walls were cleaned with a “back-scratch” tool following a high river event that caused a delay in construction;

8. The base of the shaft was cleaned with an airlift multiple times;

9. The shaft was inspected with a SoniCaliper and the base by the Shaft Inspection Device (mini-SID). The mini-SID was used to visually inspect the base because it allows downward viewing through any drilling fluid, including mineral or polymer slurry, by displacing the drilling fluid from the bell housing using pressurized nitrogen. As explained below, an unsuccessful attempt to inspect the side walls was made with a video camera, which, unlike the mini-SID, does not have means to displace the drilling fluid in the viewing area;

10. The frame containing the O-cells was placed and included the Crosshole Sonic Logging (CSL) tubes that allowed post-construction non-destructive integrity testing of the shaft. The frame was suspended such that the bottom plate was 12 inches (305 mm) above the excavation base;

11. Approximately 10 yd³ (7.6 m³) of grout was tremie placed, followed by about 12 yd³ (9.2 m³) of concrete. An attempt was then made to lower the O-cell frame into the fluid grout/concrete while still maintaining a tremie seal. However, the frame did not move once released. The final position of the bottom plate was 1 ft (0.3 m) above the socket base; and

12. Tremie placed concrete was continued throughout the remaining rock socket and a little over 3 ft (0.9 m) into the permanent casing.

The rate of penetration of the coring tool was very low at the onset, on the order of around 6 inches (150 mm) per hour, perhaps as a

result of the very high unconfined compressive strengths. However, following retrieval of the first two pieces of core, the rate of penetration increased to slightly greater than 1 ft (300 mm) per hour.

The total length of recovered rock core was approximately 25.4 ft (7.74 m), as shown in Table 1, along with the length of each of the six individual pieces. An approximation is necessary as some degree of fractured rock was present at the top of several of the recovered cores. This fractured rock may have been a result of the core extracting process.

[TABLE 1] Rock Socket Core Recovery Information

Core Recovery	Date Recovered	Length of Core Recovered
#1	May 10	~ 4.5 ft (1.36 m)
#2	May 11	~ 2.2 ft (0.67 m)
#3	May 11	~ 6.5 ft (1.98 m)
#4	May 12	~ 4.0 ft (1.22 m)
#5	May 13	~3.5 ft (1.07 m)
#6	May 13	~4.7 ft (1.43)
Total Recovered Length		~ 25.4 ft (7.74 m)

Based on weighted tape soundings and with knowledge of the permanent casing length and top elevation, a 23.3 ft (7.10 m) rock socket existed beneath the tip of the permanent casing. As noted in Table 1, the total recovered length of rock core was about 25.4 ft (7.74 m). This apparent 2.1 ft (0.64 m) discrepancy is a function of the permanent casing embedment into rock. The permanent casing was seated about 2.6 ft (0.79 m) beyond the point where it came to rest under its own weight by twisting with the Kelly bar. Presumably, the tip of the permanent casing met refusal under its own weight about 0.5 ft (0.15 m) above the top of sound rock. Therefore, the seating depth of 2.6 ft (0.79 m) was probably only around 2 ft (0.61 m) into sound rock. The observed penetration rate of the permanent casing during the seating operation serves to substantiate this observation. Hence, the cumulative measured amount of recovered rock core is in good agreement to the measured rock socket length.

Photographs of the six recovered cores are provided in Figs. 7 through 9. Fig. 10 presents a photograph of the bottom of the sixth and final piece of core that was recovered. The

base of the test shaft should be a mirror image of the rock shown in Fig. 10. The investigative core hole is visible in the photograph. The two seams in the ATV logs of Fig. 4 at elevation 311.7 ft (95.0 m) and 306.0 ft (93.3 m) correspond to the top and bottom of core number 3 at the left in Fig. 8. The dark band in the center of this core is also evident in the ATV log shown in Fig. 4.

The rock socket was inspected after final clean-out by various methods including SonicCalipers, mini-SID, side-viewing video camera, and weighted tape.

The SoniCaliper test was performed on June 2, 2010, the results of which are provided in Fig. 11. The results generally indicate a slightly oversized diameter rock socket with an average diameter of about 11.5 ft (3.51 m). This value was determined by dividing the average of the 13 perimeter measurements reported by LoadTest in the rock socket by pi. Note that an 11.5-ft (3.51-m) diameter socket agrees fairly well with back-calculated values using the concrete placement (depth-volume) records discussed below. Of special interest, the shape of the permanent casing near the tip was as estimated by the SoniCaliper is not entirely circular. This phenomenon may be the result of some sort of false-positive signal received by the tool as a result of something outside of the casing. The observed shape could also be a result of the aforementioned barge impact or deformation incurred during installation when seating the casing into rock.

The mini-SID device was used to evaluate the cleanliness of the shaft base on June 2, 2010. Five locations were viewed with the mini-SID. In general, four of the views indicated a very clean base with little or no sediment present. However, a view in the northern portion of the shaft indicated the presence of between 1.5 inches (38 mm) to 2 inches (51 mm) of sediment over the majority of the view. The mini-SID observations agreed well with weighted tape measurements. Additional air lifting was performed after the initial mini-SID inspection, but additional inspection with the device was not performed. At the onset of airlifting after the mini-SID inspection, some material was briefly observed in the discharge.

The side-wall video inspection was attempted on June 3, 2010 but was unable to see through the river water inside the casing. After several

attempts, this inspection technique was abandoned.

Careful soundings of the base were also conducted with a weighed tape throughout the coring operation and routinely thereafter. The weighted tape soundings generally indicated a clean, sound bottom around the entire base of the shaft shortly following airlifting. However, some accumulation of sediment was noticeable in the northern portion of the shaft around 1 to 2 hours after the completion of the multiple airlifting operations. While not known for certain, it is estimated that this accumulation is a result of the sediment load carried by the Mississippi River water that was used to recharge the fluid level in the permanent casing during airlifting. Because of the elevated river level, the degree of sediment load is likely increased, but is probably also high at any river stage. Admittedly, it is unclear why the accumulation appeared to only occur in the northern portion of the shaft, but one possible explanation is that the material could be deposited there as a result of the discharge direction of the recharging pump.

Another possibility is that the seal between the permanent casing and rock was compromised or never completely achieved initially, thereby allowing overburden soil (predominantly sand) to enter the excavation. However, the maintained positive head inside the permanent casing and the relatively minor amount of leakage that was observed in the fluid inside the permanent casing serves to refute this possibility. In addition, the sediment that was observed in the northern mini-SID view appeared to be fine-grained or silty, as expected if precipitated out of the fluid column.

Based on the mini-SID and weighted tape soundings, the base of the shaft was mostly free of deleterious material and was deemed acceptable.

The O-cell assembly and frame were placed on June 3. A photograph of the frame and assembly is provided in Fig. 12. The O-cell assembly consisted of four 34-inch (864-mm) diameter O-cells with a rated bi-directional capacity of 6,000 tons (53.4 MN) each for a total of 24,000 tons (213.5 MN). The top plate is 2-inches (51-mm) thick and 10.5 ft (3.20 m) in diameter. The bottom plate is also 2-inches (51-mm) thick but only 9 ft (2.74 m) in diameter. The bottom of the bottom plate is



[FIG. 7] Core Runs 1 and 2 from Test Shaft Excavation



[FIG. 8] Core Runs 3 through 5 from Test Shaft Excavation



[FIG. 9] Core Run 6 from Test Shaft Excavation



[FIG. 10] Bottom of Core Run 6 from Test Shaft Excavation

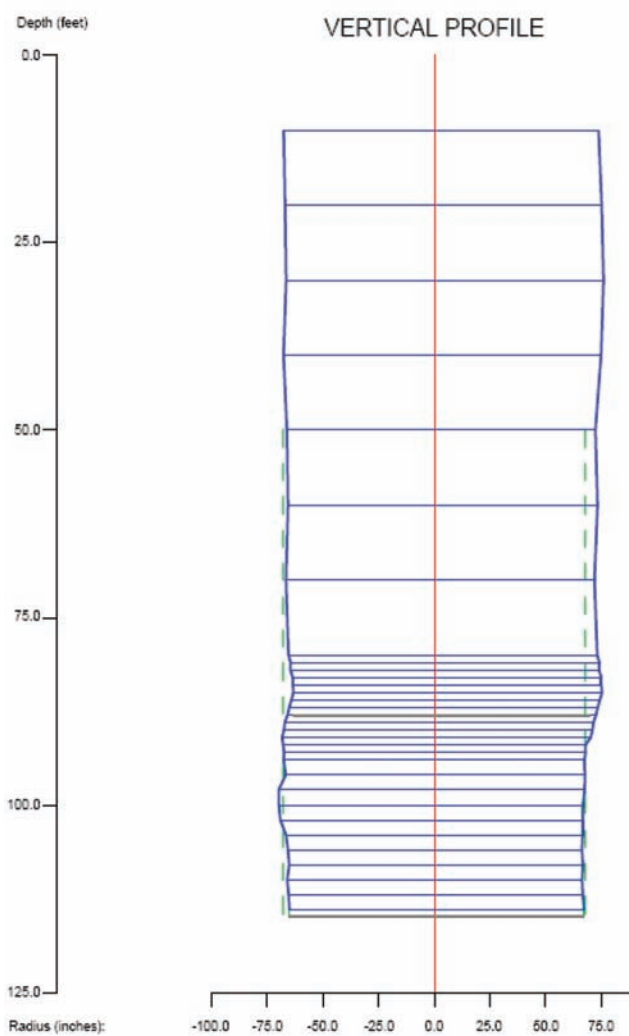


[FIG. 11] SoniCaliper Results in Test Shaft Excavation

approximately 1 ft (0.3 m) above the base of the shaft.

Three levels of four vibrating wire sister-bar strain gages, spaced at 90° are included above the top plate to estimate load shed in side resistance. Four displacement transducers and two tell tales are included to monitor movement of the plates and shaft.



[FIG. 12] O-Cell Assembly

The concrete was pumped through a 5-inch (127-mm) diameter tremie line on June 4, 2010. The tremie seal in fluid concrete or grout was never broken. The first 10 yd³ (7.6 m³) was grout followed by 96 yd³ (73.4 m³) of concrete, for a total of 106 yd³ (81.0 m³). Placement of the grout and concrete took approximately 3.5 hours. The top level of fluid concrete at the completion of the pour was 88.3 ft (26.9 m) beneath the top of the permanent casing.

The concrete employed a coarse aggregate with a 1 inch (25.4 mm) maximum particle size but about 95% of the coarse aggregate passed the

3/4 inch (19 mm) sieve. The mix included the following admixtures:

1. Type A water reducer (WR Grace Daracem 65);
2. Air entrainment (WR Grace Daravair 1400);
3. Type F high range water reducer (WR Grace Daracem ML330); and
4. Type D hydration control admixture (WR Grace Daratard 17).

One cubic yard (0.76 m³) of batch contained 546 lb (248 kg) of Type 1 cement, 182 lb (83 kg) of fly ash, 985 lb (447 kg) of fine aggregate, 1,740 lb (789 kg) of coarse aggregate, and 310 lb (141 kg) of water. After adding the High Range Water Reducer (HRWR), the maximum allowable slump was 10 inches (250 mm). Reportedly, the slump measurements at the time of the pour but prior to going through the pump were generally around 9 inches (230 mm).

Eight steel tubes for CSL purposes were also attached to the frame for subsequent testing. The ensuing CSL tests performed on June 8, 2010 indicated an apparent anomaly that was about 1 ft (0.3 m) above the top O-cell plate. While the reported anomalies could represent the presence of grout which is anticipated to have a reduced wave speed compared to concrete, it is more likely a result of the horizontal angles attached to the frame trapping less desirable material as the fluid concrete rises. These angles are apparent in Fig. 12. The presence of such members tends to trap deleterious material as the concrete rises. It was the opinion of the authors that the apparent CSL anomalies were minor and did not have any impact on the load test.

Load Test Results

The bi-directional static O-cell load test on a full-scale non-production test shaft was performed by LoadTest on June 9, 2010. A maximum bi-directional load of approximately 72,000 kips (320 MN) was applied to the shaft. The net load acting upward was 35,775 k (159 MN) and has been corrected for weight of concrete. The load acting downward was 36,067 k (160 MN). Under this load, and as shown in Fig. 13, the base of the shaft deflected downward about 0.14 inches (3.6 mm) below the O-cells and upward about the same distance above the O-cells.

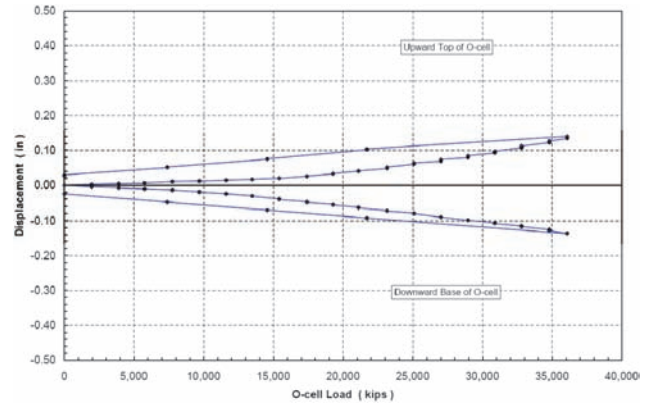


[FIG. 13] O-cell Load-Displacement (courtesy of Bill Ryan and LoadTest, Inc.)

The bi-directional load applied during the load test translates to an average unit base resistance of slightly less than 460 ksf (22 MPa) acting over a 10-ft (3.05-m) diameter base (equivalent diameter of the 9-ft (2.74-m) diameter bottom plate, 1 ft (0.3 m) above the base, projected at 2:1 angle) as shown in Fig. 14. The average unit side resistance is slightly greater than 44 ksf (2.1 MPa) acting on an 11.5-ft (3.51-m) diameter (average value from SoniCaliper and 0.5 ft (0.15 m) larger than the nominal diameter), 22.3 ft (6.80 m) long socket (measured from the bottom plate to the tip of permanent casing) as shown in Fig. 15. Note that these values were mobilized at very small displacements and do not represent the nominal strength values.

The mobilized side and base resistance in the load test exceeded the values used to develop the design in the ATC. Therefore, the load test confirmed the validity of the foundation ATC. Under purely axial loading, the production shaft rock socket lengths could have been significantly reduced. However, due to the required minimum embedment to resist lateral demand, the same socket lengths used to

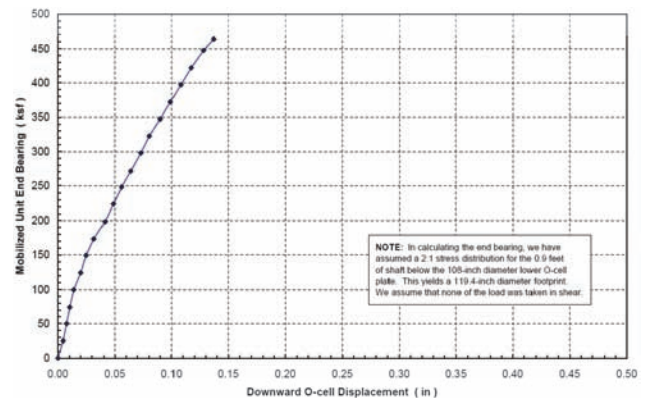


[FIG. 14] Unit Base Resistance (1 ksf = 47.9 kPa and 1 inch = 25.4 mm)

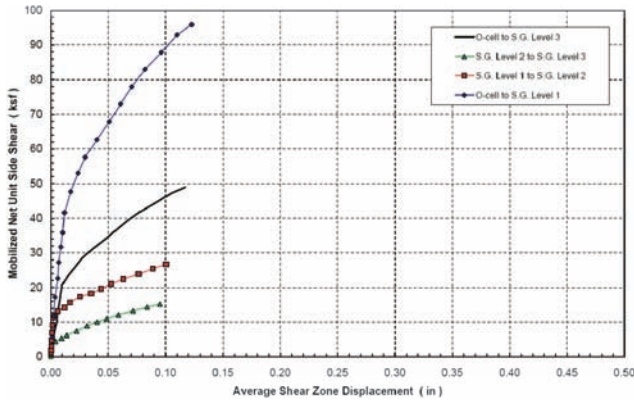


[FIG. 15] Unit Side Resistance (1 ksf = 47.9 kPa and 1 inch = 25.4 mm)

develop the ATC were maintained in the final design and constructed.

DESIGN IMPLICATIONS

The load test verified that the axial resistance of the drilled shaft in side and base resistance substantially exceeded the values used for design, and furthermore the geotechnical resistance of the rock socket exceeds the structural strength of the drilled shaft as a reinforced concrete column extending above the rock. The controlling factor for the design of the rock socket is actually the lateral and overturning loads plus the need to extend the longitudinal reinforcement to a sufficient embedment below the top of rock so that the development length requirements are satisfied. Nevertheless, it is of interest to compare the axial resistance measurements with commonly used design values.

A typical design approach for side resistance relates the unit side resistance, f_s and the square root of the unconfined compressive strength of the bedrock, $\sqrt{q_u}$. The method contained in Turner (2006) originally dating back to Horvath and Kenney (1979), and normalized to dimensionless units is presented as equation (1):

$$f_s = C(p_a)(q_u/p_a)^{1/2} \quad (1)$$

where p_a is equal to atmospheric pressure (14.7 psi or 101 kPa) and C is a constant.

The original expression of Horvath and Kenney (1979), as contained in the current edition of the FHWA Drilled Shaft Manual (Brown, Turner, and Castelli 2010), includes a constant, C , equal to 0.65. The most recent regression analysis of available load test data is reported by Kulhawy

et al. (2005) and demonstrates that the mean value of the coefficient C is approximately equal to 1.0. A lower bound value of $C = 0.63$ was shown to encompass 90% of the load test results.

The measured side resistance was less than the nominal strength value, as indicated by the data provided on Fig. 15. Therefore, any back-correlation using these measured values represents a lower bound value, since the test was limited by the capacity of the system to mobilize additional side resistance. In addition, the strength of the rock substantially exceeds the 5,000 psi (34 MPa) compressive strength of the concrete used for the drilled shaft. Traditionally, the lesser of the compressive strength of either the concrete or rock is used for design.

Based on the mobilized average unit side resistance, f_s , of approximately 44 ksf (2.1 MPa) and compressive strength, q_u , of 5,000 psi (34.5 MPa), the constant, C , from equation (1) is back-calculated to be 1.1. Using the average q_u of the rock along the length of the sockets of 24,000 psi (165 MPa), the constant, C , from equation (1) is back-calculated to be 0.5, which generally agrees with other load tests in hard limestone (Brown, 2008).

The average q_u of the rock beneath the base of the test shaft is about 12,000 psi (83 MPa) and the maximum measured unit base resistance in the load test was about 460 ksf (22 MPa). The test data shown on Fig. 14 suggest that the maximum applied pressure was well below the nominal unit base resistance. Based on a relationship between the nominal unit base resistance, q_{bN} , and the compressive strength of the rock, q_u , using equation (2):

$$q_{bN} = N_b q_u \quad (2)$$

the measured maximum applied bearing pressure suggests that the value of N_b exceeds 0.3.

The test data provide a measure of the load-deformation characteristics of the bearing formation. Using the simple relationship between the deflection, ρ_s , of a rigid circular footing bearing upon a homogeneous elastic half space, the vertical deflection under load can be estimated by the following expression:

$$\rho_s = (0.79)(q_b)(D)(1-\nu^2)/E \quad (3)$$

where: D = the diameter of the socket (10ft

projected beneath bottom plate);

ν = Poisson's ratio of the rock (estimated to be 1/4); and

E = the mass elastic modulus of the rock.

Using the maximum measured unit base resistance of 460 ksf (22 MPa) at a displacement of 0.14 inches (3.6 mm) and an unconfined compressive strength of 12,000 psi (83 MPa) beneath the base of the shaft, the value of E is back-calculated to be about 203 ksi (1,400 MPa). This value of rock mass modulus is approximately $170q_u$, a value thought to be within the typical range for sound bedrock of between $100q_u$ and $200q_u$.

CONSTRUCTION PYLON FOUNDATIONS

After completion and acceptance of the load test results, the production drilled shafts for the two pylons were completed using identical equipment and methods as for the test shaft. Each pylon foundation incorporated a two by three group of drilled shafts within the 55 by 88 ft (17 by 27 m) rectangular footprint of the foundation.

The 25 ft (7.6 m) thick footing was constructed within a sheet pile coffercell, and the soils within the coffercell were excavated to a depth of 15 ft (4.6 m) below the bottom of the footing to construct an unreinforced concrete seal slab. After tremie placement of the seal, the coffercell was dewatered to expose the top of the drilled shafts and allow the chipping of the top of the shaft to remove laitance and provide placement of reinforcement for the footing. A photo of the coffercell after dewatering is provided in Fig. 16.

CONCLUSIONS

The ATC process used on this project provided an effective mechanism for the construction team to develop an alternative foundation design that was optimized to take advantage of the capabilities of their equipment and experience. The resulting ATC design provided savings through the bidding process to the owner, and the use of load testing provided verification of the design and quality assurance to the owner.

The results of the post-award site investigation demonstrate the benefits of an intensive exploration program in terms of quality



[FIG. 16] Construction of the Pylon Foundation within Coffercell at Top of Seal

assurance and verification of conditions at each specific foundation location. Discrepancies in material properties relative to the pre-bid data were observed, but ultimately did not prove to have a major impact on the foundations at the location of the pylons. The variations in rock compressive strength were significant. The use of ATV logs within the cored exploration borings was concluded to provide useful information relative to the joints and seams in the rock as well as confirming the absence of significant solution features at the foundation locations.

The load test of the drilled shaft in hard limestone provided measurements of extremely high values of side and base resistance for the test shaft, such as to confirm that the foundation design for the subject bridge pylons was controlled by structural limitations of the reinforced concrete shaft rather than geotechnical parameters. The side and base resistance exceeded the capacity of the loading system, and nominal strength values were not mobilized during the test. A back analysis of the measured side resistance suggests that the relationships provided in the current FHWA guidelines appear to be reasonable with respect to estimating side resistance of drilled shafts in hard rock. The measured displacements below the base appear to be consistent with computed displacements of a rigid circular loading of similar size on an elastic half space having a modulus equal to approximately $170q_u$.

The CSL results and the mini-SID inspection results suggested that the load test shaft contained minor imperfections as would be typical of routine construction. The successful

load test demonstrates that sufficiently robust designs can tolerate minor imperfections.

ACKNOWLEDGEMENTS

The authors acknowledge the Missouri Dept. of Transportation as well as the contributions of Adrian Keller and Wayne Duryee of HNTB, Bill Ryan of LoadTest, Inc., and Mark Schnoebelen, John Kelley, and Tom Tavernaro of Massman Construction.

REFERENCES

1. Brown, D., Axtell, P., and Kelly, J., (2011). "The Alternate Technical Concept Process for the Foundations at the New Mississippi River Bridge, St. Louis," *Proceedings of the 36th Annual Conference on Deep Foundations, Boston*, 7p.
2. Horvath, R.G. and Kenney, T.C., (1979). "Shaft Resistance of Rock Socketed Drilled Piers." *Proceedings, Symposium on Deep Foundations*, ASCE, New York.
3. Kulhawy, F.H., Prakoso, W.A., and Akbas, S.O., (2005). "Evaluation of Capacity of Rock Foundation Sockets." *Alaska Rocks 2005, Proceedings, 40th U.S. Symposium on Rock Mechanics*.
4. Turner, J.P., (2006). NCHRP Synthesis 360: Rock-Socketed Shafts for Highway Structure Foundations. Transportation Research Board, National Research Council.
5. Brown, D.A., (2008). "Load Testing of Drilled Shaft Foundations in Limestone, Nashville, TN." Research Report for ADSC - Southeastern Chapter.
6. Brown, D.A., Turner, J.P, and Castelli, R.J., (2010). Drilled Shafts: Construction Procedures and LRFD Design Methods. FHWA NHI-10-016, May 2010.
7. Keller, A.M., (2010). "Bedrock Evaluation for Deep Foundations Utilizing an Acoustic Televiewer, I-70 New Mississippi River Bridge, St. Louis, Missouri" *Proceedings, 35th Annual Conference of The Deep Foundations Institute, Hollywood, CA*.



DFI JOURNAL

The Journal of the Deep Foundations Institute

International Standard Serial Number (ISSN): 1937-5247

Deep Foundations Institute
326 Lafayette Avenue
Hawthorne, New Jersey 07506 USA
Tel: 973-423-4030
Fax: 973-423-4031
www.dfi.org